Lab on a Chip

Chemically induced coalescence in droplet-based microfluidics†

Ilke Akartuna,‡ Donald M. Aubrecht,‡ Thomas E. Kodger‡ and David A. Weitz*

We present a new microfluidic method to coalesce pairs of surfactant-stabilized water-in-fluorocarbon oil droplets. We achieve this through the local addition of a poor solvent for the surfactant, perfluorobutanol, which induces cohesion between droplet interfaces causing them to merge. The efficiency of this technique is comparable to existing techniques providing an alternative method to coalesce pairs of droplets.

Droplet microfluidics is a promising approach for high-throughput combinatorial biological and chemical assays: each water droplet dispersed in an inert carrier fluid, typically fluorocarbon oils, acts as a small volume microreactor.[1–5] Droplets, ranging in volume from a few picoliters to nanoliters, can encapsulate aqueous reagents and isolate their contents.[6] For long-term compartmentalization of active compounds in droplets, surfactants are added to prevent coalescence. To perform many of these biological assays, reagents must be mixed with the contents of each individual droplet; this may be achieved through coalescence, where a sample droplet is paired and merged with a droplet containing new material.[7]

However, as this biologically inert oil–water interface is nearly always stabilized with surfactants, targeted coalescence becomes challenging. Despite the surfactant-induced stability, several experimental methods have been developed to controllably coalesce droplet pairs. Partially stable droplets with a minimal surfactant concentration have been coalesced using abrupt changes in surface area.[8,9] By contrast, coalescence of fully stabilized droplets has only been achieved using external stimuli: electro-coalescence or optical heating.[7,10–13] Electro-coalescence involves merging of droplet pairs by applying an electric field as droplets pass through a confining region of a microfluidic channel bordered by fabricated electrodes. Optical heating of droplet interfaces involves using a focused laser to locally change the temperature and the surface tension of the droplet interfaces. However, there are instances where neither an electric field nor optical heating can be applied, thus the development of a simple and robust tool for performing controlled droplet coalescence would be beneficial.

In this paper, we present a new microfluidic method to coalesce a stream of paired surfactant-stabilized water-in-fluorocarbon

School of Engineering and Applied Sciences, Harvard University, 29 Oxford Street, Cambridge, USA. E-mail: weitz@seas.harvard.edu

oil droplets. The local addition of a poor solvent for the surfactant, perfluorobutanol, induces cohesion between paired droplet interfaces, the droplets merge and coalesce. Then the alcohol is diluted to restabilize the droplets. To elucidate the mechanism that leads to coalescence, we determine the surfactant solubility and, by measuring the static interfacial tensions and the droplet contact angles at different proportions of alcohol, we determine the strength of the cohesion between droplets. We show that the merging efficiency of this chemical coalescence method is comparable to electro-coalescence of droplets.

To coalesce a bulk emulsion of aqueous droplets in fluorinated oil, a concentration of 20 vol% perfluorooctanol, PFO, is typically used to lower the stability of the interfaces by possibly displacing the surfactant at the interface;[14] however, breaking the emulsion requires a combination of vigorous mixing and centrifugation both of which are not possible on-chip. Instead, we use perfluorobutanol, PFB, which results in bulk coalescence with no mixing or centrifugation. Eliminating the necessity for mechanical agitation provides a path where a sample droplet can be passively coalesced with a second droplet containing new reagent inside a microfluidic channel.

For our experiments, we use a flow focusing geometry to produce 40 μm droplets, labeled green, while simultaneously reinjecting pre-formed 25 μm droplets, labeled red. Each droplet stream enters one side of a Y-junction as shown in Fig. 1A.[15] Synchronization between droplet streams is achieved by controlling the flow rate of each stream using syringe pumps. Small pressure fluctuations as the larger droplets enter the exit channel, force the reinjected smaller droplets to slowdown and then follow the large droplets out the exit channel of the Y-junction, enhancing synchronization.[5] The droplets must now touch, or pair. A long straight channel is added after the Y-junction to allow the smaller droplets to catch up to the larger droplets; the smaller droplets sample less of the flow profile and thus experience a higher average velocity.[7] Successfully paired droplets may now be coalesced.
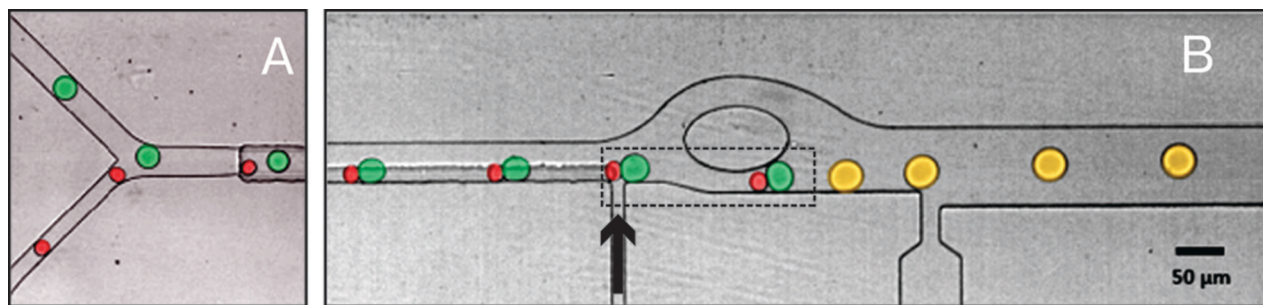
Fig. 1 Passive microfluidic droplet coalescence through the addition of a destabilizing alcohol; the flow direction is from left to right. (A) Upstream pairing of two different size droplets labeled with rhodamine–dextran (red, small) and fluorescein–dextran (green, large). (B) Perfluorobutanol is added through the channel indicated by the black arrow, causing downstream coalescence of paired droplets. Dashed box region is magnified in Fig. 3. Droplets are false colored.

However, for this on-chip chemically-mediated coalescence to occur, paired droplets must interact with an incoming PFB stream. Fluid additions at low Reynolds number, as in microfluidic devices, will divert streamlines and push droplets away from any incoming stream.† To steer droplets across streamlines to the lower wall where the PFB is introduced from a side channel, we modify the long straight channel. By adding an 8 μm tall tapering feature to the channel ceiling, buoyant aqueous droplets fill this additional volume and are steered by the taper to the lower channel wall as seen in Fig. 2A. By contrast, in a simple rectangular cross-section channel, droplets remain centered as shown in Fig. 2B. We quantify the steering by measuring the center of each droplet as it flows along the microfluidic channel as shown in Fig. 3C; the droplet centers move 8 μm toward the lower wall and the incoming PFB stream.

Droplet pairs now exit the steering channel and directly contact a stream of PFB for ~1.30 ms, as shown by black arrows in Fig. 3A–C. The paired droplets pass through a constriction in ~2.6 ms as shown in Fig. 3D–G; upon exiting, the velocity of the leading green large droplet rapidly decreases, forcing the droplet pairs into close contact and then to quickly coalesce, as shown in Fig. 3H, I. Once coalesced, the dye from the red and green droplets mix yielding single yellow droplets which flow downstream where the PFB is diluted with continuous phase added through the large side channel shown in Fig. 1B. No more coalescence events are seen after this dilution as the yellow droplets are restabilized due to a drop in PFB concentration. We simply collect the merged droplets off-chip for additional steps. This entire process proceeds at approximately 300 droplet merging events per second comparable to the rates of electro-coalescence methods.[3,5,7] This merging rate is typically limited by imperfect upstream pairing; at higher rates, both droplet streams are difficult to synchronize with 'extra' droplets being incorporated, resulting in triplets.

Interestingly, as paired droplets contact a stream of PFB added at 10 μL h^{-1}, they appear to adhere strongly to the channel wall as indicated by black arrows in Fig. 3. When the droplet pairs first contact PFB, a concentration gradient enhances local adhesion. Surprisingly, adhesion and coalescence are absent when PFO is flowed instead of PFB in the microfluidic device operation described above, up to flow rates of 500 μL h^{-1}. Similarly, adding fluorocarbon oil instead of PFB yields no coalescence events; device geometry alone is insufficient to account for the adhesion or coalescence.[16]
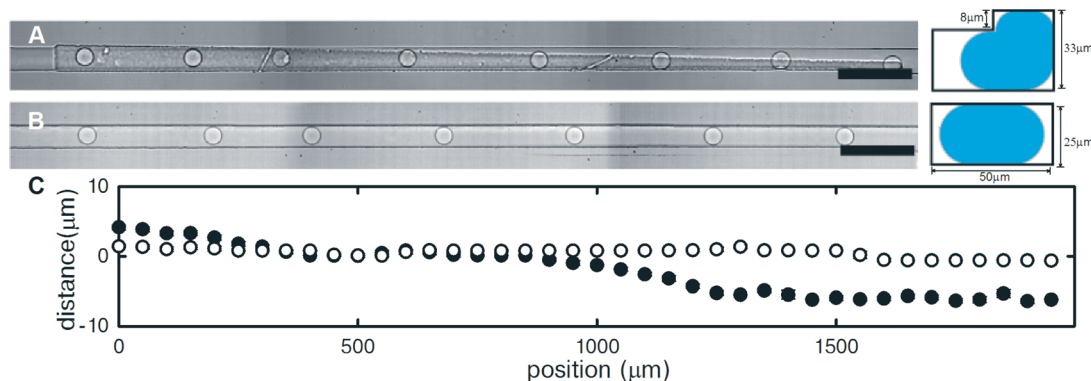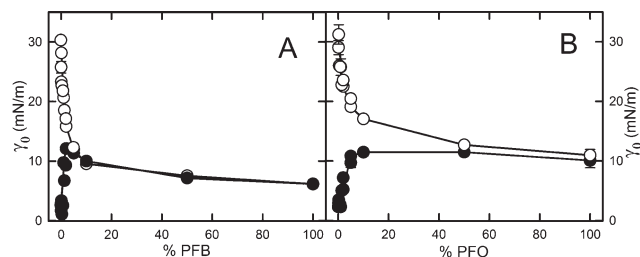

Fig. 2 Droplets steering channel. (A) Droplets passing though a 50 μm wide, 25 μm tall channel. A schematic of the channel cross-section is shown at right, with the droplet volume represented in blue. (B) Droplets passing though a steering microfluidic channel. The primary channel has the same dimensions as (A), but has a tapering 8 μm tall feature added on the ceiling. Scale bar is 150 μm. (C) Average droplet center position in the channel as a function of droplet position along the flow direction; (○) without steering-ceiling, (●) with steering-ceiling. 0 on the y-axis corresponds to the channel center-line.
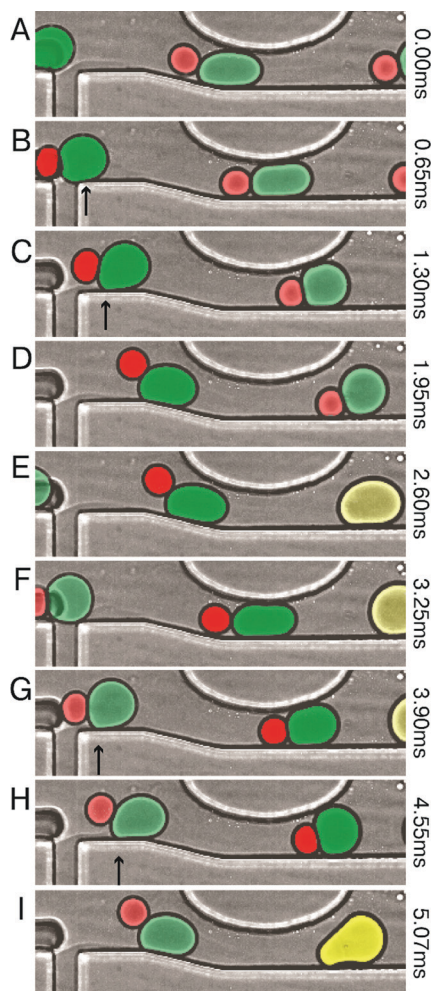
Fig. 3 Droplet pairs contacting the PFB stream (A–C), passing through the constriction (D–H) and coalescing (I). Wall adhesion is marked by black arrows. Flow rate for PFB addition is 10 μL h^{-1}. Droplets are false colored.


Fig. 4 Equilibrium interfacial tensions, γ_0, as a function of alcohol concentration from pendant drop and DuNouy ring measurements for (A) perfluorobutanol (PFB) and (B) perfluorooctanol (PFO) with (●) 2 wt% surfactant, (○) no surfactant.

Clearly, the interaction between the PFB and the paired droplets is playing a crucial role in the observed adhesion and subsequent coalescence. While it is difficult to determine the origin of this adhesion inside the device, we can perform bulk experiments to elucidate the mechanism.

To understand the effects of PFB on the interface, we measure the interfacial tension, γ_0, for the local solution conditions encountered within the microfluidic device using both pendant drop and DuNuoy ring techniques. In the absence of surfactant, increasing the volume fraction of PFB causes an abrupt decrease in the interfacial tension from $\gamma_0 = 32$ mN m^{-1}, for the clean water–fluorinated oil interface, to $\gamma_0 = 15$ mN m^{-1} at only 2 vol% PFB as seen in Fig. 4A. Similarly, in the absence of PFB, adding 2 wt% surfactant to the bare interface also results in a large decrease in the interfacial tension, $\Delta\gamma_0$ ~30 mN m^{-1}. Interestingly, upon addition of PFB to this surfactant-laden interface, the interfacial tension rises sharply as seen in Fig. 4A. At concentrations >2 vol% PFB, there is no measurable difference in interfacial tension between surfactant-free and surfactant-laden interfaces, suggesting that the

surfactant no longer stabilizes the interface. This effect is absent for identical measurements made with PFO: the interfacial tension difference for surfactant-free and surfactant laden interfaces is not zero until >50 vol% PFO as seen in Fig. 4B.

To resolve this stark contrast in interfacial behavior between two seemingly similar alcohols, we examine the bulk phase equilibrium of fluorocarbon oil with 2 wt% surfactant at different concentrations of PFB and PFO. Once the oil phase reaches 85 vol% PFB, the sample becomes turbid as the surfactant precipitates out of solution. By contrast, the surfactant is soluble at 2 wt% at all concentrations of PFO. Crucially, it is this precipitation that causes the cohesive nature of surfactant-stabilized droplet interfaces. By locally adding a poor solvent for the surfactant, we are able to induce cohesion between fluid interfaces causing rapid draining of the thin liquid film between droplets and rendering the interfaces highly susceptible to coalescence.[8,16]

This cohesion is first seen as adhesion to the microfluidic channel walls which are coated with surfactant as seen in Fig. 3. We quantify the strength of adhesion at different concentrations of PFB and PFO by measuring the contact angle made by a single droplet and a surfactant-coated PDMS surface using 3D confocal microscopy, schematically shown in Fig. 5A. Imaging a fluorescent aqueous droplet labeled with FITC–dextran at the droplet equator yields the droplet diameter as seen in upper images of Fig. 5B. Simultaneously, we measure the diameter of the adhesive contact area using
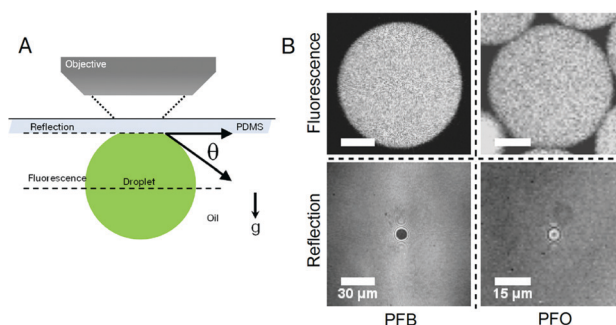
Fig. 5 Measuring droplet adhesion. (A) Schematic of upright confocal experiment. (B) 2D confocal slices from the reflection and fluorescence channel. Reflection signal at the PDMS-droplet interface plane and fluorescence at the mid-plane of a droplet in 10 vol% PFB (left) and 10 vol% PFO (right).

confocal reflection microscopy where a dark patch appears at the PDMS-droplet interface, akin to black spots in thin films as seen in lower images of Fig. 5B. Using these two diameters, the adhesive contact angle, θ, is calculated geometrically and shown as a function of alcohol concentration in Fig. 6A. Combined with the previously measured equilibrium surface tensions, γ_0, we determine the energy of adhesion, ΔF, as a function of alcohol concentration using $\Delta F = 2\gamma_0(1 - \cos(\theta))$.[17] We find that the energy of adhesion for interfaces exposed to PFB quickly increases at ~5 vol% as shown in Fig. 6B. By contrast, the energy of adhesion for interfaces exposed to PFO is comparably low up to ~50%, then rises gradually, as shown in Fig. 6B. Both results are in excellent agreement with a cohesion-based coalescence between droplets in the presence of PFB and the surfactant remaining soluble at all concentrations of PFO.

While 5 vol% PFB is required to induce cohesion and coalescence of a single droplet pair, multiple downstream coalescence events must be prevented for microfluidic assays. We achieve this by reducing the concentration of PFB immediately after the coalescence; droplet interfaces are restabilized by eliminating the cohesion. After a single droplet pair coalescence event, we introduce a new stream of PFB-free continuous phase in the microfluidic device, lowering the final PFB concentration to <1 vol%. By diluting the PFB, merged and then restabilized droplets can be collected from the device outlet continuously.

To determine the efficiency of this chemical coalescence process on the microfluidic chip, we count droplet merging events recorded in high-speed movies. If drops are successfully paired, greater than 96% are successfully merged; this is nearly as efficient as electro-coalescence of droplets.†[5,7,12] However, undesired coalescence events between more than two droplets occur. These 'extra' droplets are typically a result of imperfect upstream pairing; an excess number of small droplets may enter the coalescence region of the device with a droplet pair, forming a triplet. We observe that the oblate post in this microfluidic device diverts most of the single droplets to the top channel away from the constriction zone, avoiding triplets. Additionally, when three droplets do enter the constriction region of the device, we do not observe all three droplets coalescing; such events are inherently prevented as all three droplet interfaces must be in contact for chemical

coalescence to proceed. By contrast, as the electric field interaction in microfluidic electro-coalescence is long ranged compared to the size of a droplet pair, multiple droplets may be driven together and coalesced.[5,7]

Conclusions

In this work, we report a method to coalesce droplets through the local addition of PFB, yielding interfacial cohesion between surfactant-stabilized droplet pairs in a microfluidic device. This new method for coalescing otherwise perfectly stable droplets inside a microfluidic device is an alternative to the use of electric fields[5,7,10,12] and optical heating.[13] The absence of electric field may be beneficial for certain biological assays where electroporation[18,19] or cell lysis of fragile cells[20,21] must be avoided. This method simplifies on-chip droplet coalescence as it requires no electrodes or additional instrumentation such as the electronics to control electrodes or the sensitive alignment of lasers.

Materials and methods

Microfluidic channels are fabricated with poly-dimethylsiloxane (PDMS) using standard soft lithography protocols.[22,23] The fluidic channel mold is fabricated *via* photo-lithography and chemical development of SU-8 photoresist (Microchem). Sylgard 184 PDMS (Dow Corning) is mixed at the standard 1:10 mass ratio, poured over the mold, degassed for 20 minutes under vacuum, and cured at 65 °C for 18 hours. After curing, the PDMS replica is removed from the mold, fluid inlet holes formed with a biopsy punch, and the PDMS piece bonded to glass using oxygen plasma treatment.[24] The microfluidic channels are treated with a fluorophillic silane, Aquapel (Ryder Fleet Products) by flowing through the channels for 30 seconds, and then flushed out with Novec HFE-7500 (3M) fluorocarbon oil.

Unless otherwise noted, the dispersed phase for all experiments is DI water. The continuous phase is Novec HFE-7500 with additional components, as noted. Aqueous droplets are stabilized using 2 wt% PFPE-PEG-PFPE triblock copolymer surfactant[25] dissolved in the fluorocarbon continuous phase, at roughly 2.5X times the CMC. 2,2,3,3,4,4,4-Heptafluoro-1-butanol (PFB, Oakwood Products) is used to induce droplet coalescence.

Prior to a droplet coalescence experiment, one droplet population is formed in a flow-focusing design microfluidic channel with a droplet nozzle cross-section of 15 μm × 15 μm. 25 μm droplets are created using flow rates of 180 μL h^{-1} and 100 μL h^{-1} for the continuous and dispersed phases, respectively. Droplets are collected into a 1 mL plastic syringe (Becton Dickinson). These droplets are used as the reinjected droplet population during coalescence experiments.

Droplet coalescence experiments are performed using the Y-channel. From the lower arm of the Y, we reinject 25 μm droplets at 15 μL h^{-1} and space them with HFE-7500 flowing at 150 μL h^{-1}. From the opposite arm of the Y, 40 μm droplets are formed at a flow-focusing nozzle using a dispersed
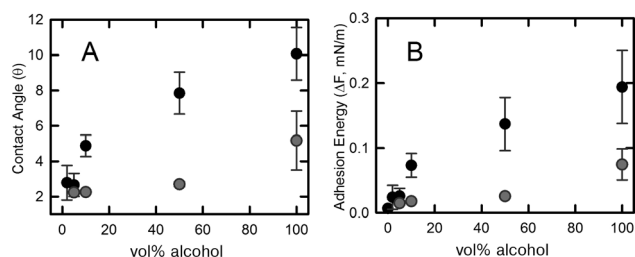
Fig. 6 (A) Measured contact angle between surfactant coated surfaces and droplets as a function of fluorinated alcohol concentration; (●) perfluorobutanol (PFB) and (◉) perfluorooctanol (PFO). (B) Calculated adhesion energy, ΔF, using the equation in the text.

phase flow rate of 40 μL h^{-1} and a continuous phase flow rate of 300 μL h^{-1}. In the coalescence region of the device, 100% PFB is injected into the continuous phase at 10 μL h^{-1}. Other flow rates have been tested and >20 μL h^{-1} resulted in multiple coalescence events and <10 μL h^{-1} yielded very few coalescence events. Coalesced droplets are restabilized by adding fresh HFE-7500 at 500 μL h^{-1} to dilute the final PFB concentration. See ESI† for complete device drawing.

Interfacial tension measurements are performed on two instruments. Equilibrium measurements are made on a KSV Sigma 701 tensiometer (Biolin Scientific) with a platinum DuNouy ring; the ring is rendered fluorophilic by silanization in 1 vol% 1H,1H-2H,2H-perfluorodecyl trichlorosilane (Sigma) in HFE-7500. Dynamic and equilibrium measurements are also made using a custom pendant drop instrument. The pendant drop instrument captures digital images at frame rates up to 15 fps and calculates the interfacial tension values using a curve fitting route in Matlab to match the droplet interface profile.[26,27] Values from this pendant drop instrument are verified against values calculated by a commercial KSV CAM 200 pendant drop surface tension meter (Biolin Scientific).

Adhesion measurements are performed in droplet imaging chambers. The chambers are fabricated by sandwiching 1 mm thick glass spacers between a standard microscope slide and a glass coverslip coated with a thin layer of ~20 μm Sylgard 184 to mimic the microfluidic channel wall. This sandwich is glued together using NOA 81 (Norland Products, Inc) and exposed to UV. Chambers are immersed in Aquapel, dried with compressed air, and then soaked for 5 minutes in a solution of 2 wt% PFPE-PEG-PFPE in HFE-7500 to guarantee surfactant adsorption on the interior of the chamber. The chamber is then removed from the surfactant solution, dried with compressed air, and all but one side sealed using 5 minute epoxy. Once the epoxy is cured, the chamber is filled with the appropriate test solution, then droplets containing 0.5 mg mL^{-1} dextran–fluorescein are pipetted into the test solution. Adhesion is quantified by recording simultaneous 3D confocal image stacks of the fluorescence and reflection signals.

Acknowledgements

References

1 S. Koester, F. E. Angile, H. Duan, J. J. Agresti, A. Wintner, C. Schmitz, A. C. Rowat, C. A. Merten, D. Pisignano, A. D. Griffiths and D. A. Weitz, *Lab Chip*, 2008, **8**, 1110.

2 Y. Schaerli and F. Hollfelder, *Mol. BioSyst.*, 2009, **5**, 1392.

3 J. J. Agresti, E. Antipov, A. R. Abate, K. Ahn, A. C. Rowat, J.-C. Baret, M. Marquez, A. M. Klibanov, A. D. Griffiths and D. A. Weitz, *Proc. Natl. Acad. Sci. U. S. A.*, 2010, **107**, 4004–4009.

4 M. T. Guo, A. Rotem, J. A. Heyman and D. A. Weitz, *Lab Chip*, 2012, **12**, 2146.

5 E. Brouzes, M. Medkova, N. Savenelli, D. Marran, M. Twardowski, J. B. Hutchison, J. M. Rothberg, D. R. Link, N. Perrimon and M. L. Samuels, *Proc. Natl. Acad. Sci. U. S. A.*, 2009, **106**, 14195–14200.

6 J.-C. Baret, *Lab Chip*, 2012, **12**, 422.

7 K. Ahn, J. Agresti, H. Chong, M. Marquez and D. A. Weitz, *Appl. Phys. Lett.*, 2006, **88**, 264105.

8 L. G. Leal, *Phys. Fluids*, 2004, **16**, 1833.

9 N. Bremond, A. Thiam and J. Bibette, *Phys. Rev. Lett.*, 2008, **100**, 024501.

10 C. Priest, S. Herminghaus and R. Seemann, *Appl. Phys. Lett.*, 2006, **89**, 134101.

11 A. Thiam, N. Bremond and J. Bibette, *Phys. Rev. Lett.*, 2009, **102**, 188304.

12 M. Zagnoni, G. Le Lain and J. M. Cooper, *Langmuir*, 2010, **26**, 14443–14449.

13 C. N. Baroud, M. Robert de Saint Vincent and J.-P. Delville, *Lab Chip*, 2007, **7**, 1029.

14 A. B. Theberge, E. Mayot, A. El Harrak, F. Kleinschmidt, W. T. S. Huck and A. D. Griffiths, *Lab Chip*, 2012, **12**, 1320.

15 S. L. Anna, N. Bontoux and H. A. Stone, *Appl. Phys. Lett.*, 2003, **82**, 364.

16 A. R. Thiam, N. Bremond and J. Bibette, *Langmuir*, 2012, **28**, 6291–6298.

17 P. Poulin and J. Bibette, *Langmuir*, 1998, **14**, 6341–6343.

18 T. Geng and C. Lu, *Lab Chip*, 2013, **13**, 3803.

19 Y. Zhan, J. Wang, N. Bao and C. Lu, *Anal. Chem.*, 2009, **81**, 2027–2031.

20 H. Lu, M. A. Schmidt and K. F. Jensen, *Lab Chip*, 2005, **5**, 23.

21 J. T. Nevill, R. Cooper, M. Dueck, D. N. Breslauer and L. P. Lee, *Lab Chip*, 2007, **7**, 1689.

22 Y. Xia and G. M. Whitesides, *Angew. Chem., Int. Ed.*, 1998, **37**, 550–575.

23 J. C. McDonald, D. C. Duffy, J. R. Anderson, D. T. Chiu, H. Wu, O. J. A. Schueller and G. M. Whitesides, *Electrophoresis*, 2000, **21**, 27–40.

24 M. K. Chaudhury and G. M. Whitesides, *Langmuir*, 1991, **7**, 1013–1025.

25 C. Holtze, A. C. Rowat, J. J. Agresti, J. B. Hutchison, F. E. Angile, C. H. J. Schmitz, S. Koester, H. Duan, K. J. Humphry, R. A. Scanga, J. S. Johnson, D. Pisignano and D. A. Weitz, *Lab Chip*, 2008, **8**, 1632.

26 Y. Rotenberg, L. Boruvka and A. Neumann, *J. Colloid Interface Sci.*, 1983, **93**, 169–183.

27 Y. Touhami, G. H. Neale, V. Hornof and H. Khalfalah, *Colloids Surf., A*, 1996, **112**, 31–41.